Neuron, Vol. 18, 539–551, April, 1997, Copyright ©1997 by Cell Press

TWH Regulates the Development of Subsets of Spinal Cord Neurons

Changlin Dou,*§ Xin Ye,†§ Colin Stewart,‡ Eseng Lai,* and Suzanne C. Li†
*Cell Biology Program and Division of Endocrinology
Memorial Sloan-Kettering Cancer Center
New York, New York 10021
†Department of Pediatrics
Columbia University
New York, New York 10032
‡Advanced BioScience Laboratories, Inc.
Basic Research Program
Frederick, Maryland 21702

Summary

Thymocyte winged helix (TWH) is a putative transcription factor expressed in the developing neural tube. At midgestation, TWH expression identifies subsets of spinal cord motor neurons and interneurons. TWH-expressing motor neurons were restricted to specific spinal cord levels, distinguishing motor neurons at lumbar from those at cervical levels. To understand the developmental role of TWH, we replaced the TWH gene with the lacZ reporter gene and generated mice with a homozygous disruption of the TWH gene. TWH$^{(-/-)}$ mutant mice had increased perinatal mortality, retarded postnatal growth, and motor weakness. The TWH$^{(-/-)}$ mutation resulted in alterations in the sizes and position of different neuronal populations. Our results demonstrate that TWH plays a critical role in neuronal development and suggest that TWH regulates the early differentiation of neural progenitors.

Introduction

Motor neurons, and the other cell types of the central nervous system, arise from the neuroepithelium through a process that is regulated spatially and temporally. Inductive signals and modifiers, provided by adjacent tissues, pattern the neuroepithelium along the anteroposterior (A–P) and dorsoventral axes (reviewed by McConnell, 1995; Lumsden and Krumlauf, 1996; Tanabe and Jessell, 1996). These signals progressively restrict the developmental potential of the progenitor cell. Within the spinal cord, motor neurons are the first major class of neurons born. The number of motor neurons generated and their birth dates are relatively fixed for a given species (reviewed by Hollyday, 1980).

Shortly after their generation, motor neurons settle to specific positions within the spinal cord. Motor neurons are organized into longitudinal columns that extend along the A–P axis. Those that innervate axial muscles form a ventromedial column of motor neurons (medial motor column [MMC]), while those that innervate limb muscles form a ventrolateral column of motor neurons (lateral motor column [LMC]) at limb levels. Each column is subdivided into a medial and lateral division (MMCm, MMCl, LMCm, and LMCl), based on the dorsal or ventral origin of the target muscle (reviewed by Landmesser, 1980). Within each of these major motor column subsets, groups or pools of motor neurons are found. Each pool represents the neurons that innervate an individual target muscle (Hollyday, 1980; reviewed by Landmesser, 1980). Motor function requires the establishment of accurate connections between motor neurons and their target muscles (reviewed by Landmesser, 1980; Eisen, 1994). The axons of all motor neurons exit together from the spinal cord via the ventral roots. Different pathways are then selected by the different motor neuron subsets. Recent studies suggest that the initial axonal trajectories may be specified by members of the LIM homeobox transcription factor family (Tsuchida et al., 1994; Tosney et al., 1995). These genes are expressed before selection of the axonal pathway occurs, and the different major motor column subsets express distinct combinations of these proteins (Tsuchida et al., 1994; Appel et al., 1995). Additional genes may function in the selection of the subsequent pathway choices required to reach individual target muscles.

Many members of the winged helix (WH) family of transcription factors have been found to play critical roles in invertebrate and vertebrate development (reviewed by Lai et al., 1993). *slp1* and *slp2* are important for segmentation of the Drosophila embryo (Grossniklaus et al., 1992), and HNF-3β is essential for the formation of the murine node and notochord (Ang and Rossant, 1994; Weinstein et al., 1994). Some members, such as the C. elegans gene *lin-31*, regulate cell fate within the WH-expressing cell (Miller et al., 1993). Other members play important roles in inductive interactions between tissues. BF-2 is expressed in the kidney stroma and regulates the differentiation of the adjacent nephrogenic mesenchyme (Hatini et al., 1996). We have identified a WH transcription factor, thymocyte winged helix (TWH), that displays a changing pattern of expression in the developing central nervous system. TWH is initially widely expressed in the neuroepithelium. By midgestation, TWH expression is restricted to subregions of the brain and spinal cord. To determine the role of TWH in spinal cord development, we examined the expression of TWH within the spinal cord in mice with a targeted lacZ transgene driven by the TWH promoter. The expression of the lacZ gene marks a population of motor neurons and ventral interneurons normally expressing TWH, which we refer to as TWH active-promoter (TAP) neurons. TAP motor neurons comprise distinct subsets of motor neurons of both the medial and lateral motor columns. These subsets are restricted to specific A–P levels, suggesting that they may represent specific motor neuron pools. We find that TWH is essential for normal motor function, as TWH$^{(-/-)}$ mutant mice have motor weakness. The TWH$^{(-/-)}$ mutation affected the size of the spinal cord TAP neuronal populations, as well as at least one non-TAP neuronal population. Our studies suggest that TWH plays a critical role during the early differentiation of the spinal cord neural progenitor cell.

§ These authors contributed equally to this work.

Results

The TWH Gene Is Expressed in the Developing Central Nervous System

TWH was initially identified from a thymus cDNA library by low stringency hybridization, using a WH binding domain probe (from HNF-3α) (Li et. al., unpublished data). The DNA binding domain of TWH is identical to the published partial sequence of Mf3 (Sasaki and Hogan, 1993), HFH–E5.1 (Ang et al., 1993), and *fkh*-5 (Kaestner et al., 1993). The full-length sequence of *fkh*-5 has recently been reported (Kaestner et al. 1996) and is 95% identical to the sequence of TWH. TWH expression was found to be restricted to thymocytes and the central nervous system by RNA analyses of tissues and cell lines. To identify the specific cells within the central nervous system that express TWH, in situ hybridization studies were performed on $TWH^{(+/+)}$ (wild-type, WT) tissues. At E12.5, TWH expression was restricted to specific groups of cells in the posterior diencephalon, midbrain, hindbrain, and spinal cord. In the brain, the highest levels of expression were found in the mammilary body of the hypothalamus, the superior and inferior colliculi, and some of the cranial nerve ganglia (Figures 1A and 1D; data not shown). In the E14.5 spinal cord, TWH was expressed in a subset of ventral cells and in cells surrounding the central canal (Figure 1G). In situ analyses of HFH-E5.1 and *fkh*-5 showed that it is expressed in the neural ecto- and mesoderm of E7.0–E7.5 embryos (Ang et al., 1993; Kaestner et al., 1996). By midgestation (E12.5–E13.5), HFH-E5.1 and *fkh*-5 expression are restricted to cells in the hypothalamus, midbrain, medulla oblongata, and ventral spinal cord. The expression pattern of TWH raised the possibility that it has an important function in neural development.

Targeting of lacZ to the TWH Promoter and Generation of $TWH^{(-/-)}$ Mutant Mice

To examine the function of TWH, we generated mice in which we replaced the TWH gene with the lacZ gene that encodes E. coli β galactosidase. A deletion of 60% of the coding sequences, including all of the DNA binding domain, was generated by homologous recombination in embryonic stem (ES) cells with positive–negative selection (Figure 2) (Kontgen and Stewart, 1993). The TWH sequences were replaced with a lacZ cassette containing a nuclear localization signal (Moynahan et al., 1996). The lacZ gene was fused to the 5′ untranslated region of the TWH gene so that its expression would be regulated by the TWH promoter. From 80 G418 and FIAU doubly resistant ES cell clones, 5 had undergone homologous recombination to disrupt the TWH gene. One of these clones was injected into C57bl/6 blastocysts, giving rise to male chimeras that transmitted the mutant allele thru the germ line. The mutant allele was maintained in a hybrid 129/C57bl/6 background. Mice heterozygous for the TWH mutation appeared normal in terms of growth, behavior, fertility, and viability. $TWH^{(+/-)}$ heterozygous mice were intercrossed to generate $TWH^{(-/-)}$ mutant mice.

The lacZ Marker Is a Faithful Reporter of TWH Expression

We compared the pattern of β-galactosidase activity in $TWH^{(+/-)}$ heterozygous embryos to that of TWH expression by in situ hybridization in WT embryos to determine whether lacZ expression reliably reports the activity of the TWH promoter. Figure 1 shows that the pattern of β-galactosidase activity in E12.5 $TWH^{(+/-)}$ heterozygous midbrain matched the expression pattern of TWH RNA in the E12.5 WT midbrain (Figures 1B versus 1A). Similarly, the pattern of β-galactosidase activity in E14.5 $TWH^{(+/-)}$ heterozygous hypothalamus and spinal cord tissues matched the expression of TWH RNA in these WT tissues (Figures 1E and 1H versus 1D and 1G). A comparable pattern of β-galactosidase activity and TWH expression was found in all other sites in the developing embryo, including the superior and inferior colliculi and cranial nerve ganglia (data not shown). Thus, β-galactosidase activity in the $TWH^{(+/-)}$ heterozygote accurately reflects the normal pattern of TWH expression during development. Because detection of β-galactosidase activity provides greater resolution than in situ hybridization studies, we have used the lacZ marker to study the expression pattern of TWH in phenotypically normal $TWH^{(+/-)}$ heterozygous mice. The lacZ marker enables us to examine cells that have a transcriptionally active TWH promoter in the $TWH^{(+/-)}$ heterozygote, compared with the same population in the $TWH^{(-/-)}$ mutant. We refer to cells that express β-galactosidase activity in the $TWH^{(+/-)}$ heterozygote and $TWH^{(-/-)}$ mutant as TAP cells.

TWH Expression Identifies a Subpopulation of Spinal Cord Motor Neurons and Interneurons

At E18.5, two longitudinal columns of TAP cells were found to traverse the entire ventromedial spinal cord. Two more columns of TAP cells were found in the ventrolateral spinal cord at lumbar levels (Figure 3A). The TAP cells in these ventral columns were concentrated in the most ventral portion of the ventral horn; had large, ovoid nuclei; and were identified as neurons in double-labeling immunohistochemistry studies (Figures 3C, 3E, and 3G; data not shown). These cells expressed a neuron-specific marker (cyn-1) and did not express glial markers (GFAP or nestin). All of the ventrolateral TAP neurons expressed acetylcholinesterase activity and were therefore identified as motor neurons (data not shown). These TAP motor neurons formed a subset of the lateral motor column (LMC). In contrast, only a subset of the ventromedial TAP neurons were motor neurons and appeared to form a subset of the medial motor column (MMC) (Figure 3G). The remaining ventromedial TAP neurons most likely represent ventral interneurons.

Additional TAP cells lined the central canal; these appeared to represent ependymal cells (Figures 3C and 3E). Other TAP cells with small narrow nuclei were found in the dorsal spinal cord (Figures 3C and 3E). None of these small TAP cells stained for neuronal markers; a subset stained for the glial markers GFAP and/or nestin (data not shown). No panglial marker is available, but

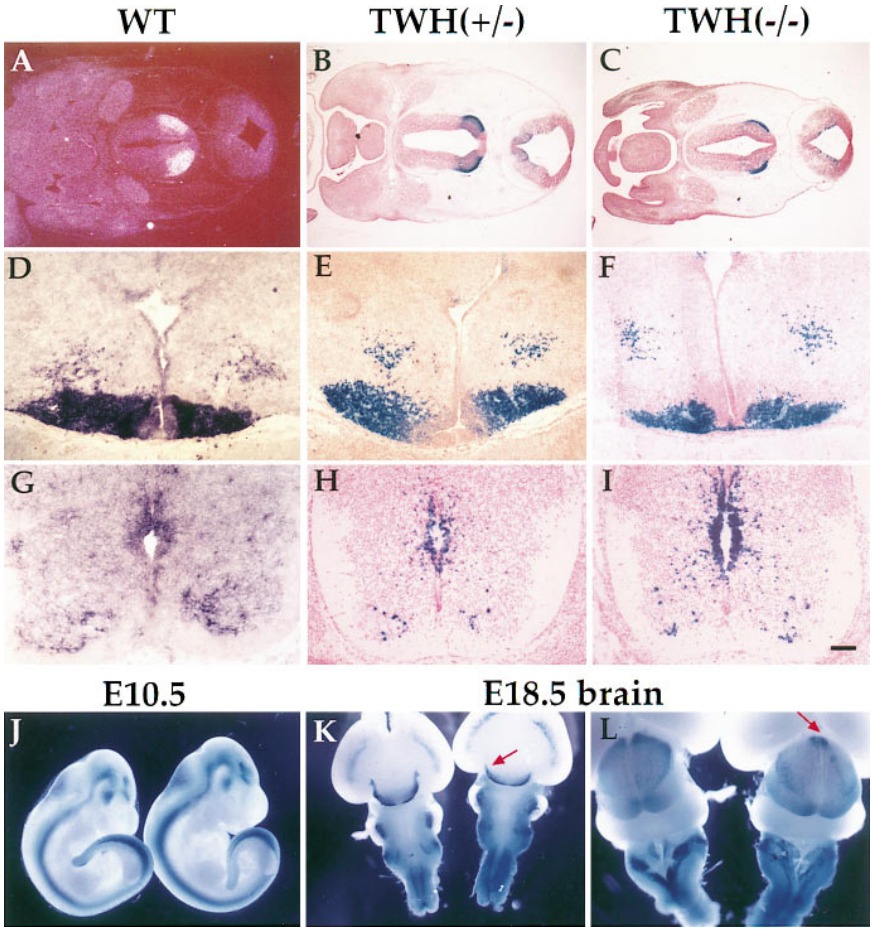

Figure 1. The lacZ Marker Is a Faithful Reporter of TWH Expression in the TWH$^{(+/-)}$ Heterozygote

Expression of the TWH gene was determined by in situ hybridization in WT tissues ([A], [D], and [G]) and compared to the pattern of β-galactosidase activity in TWH$^{(+/-)}$ heterozygote ([B], [E], and [H]) and TWH$^{(-/-)}$ mutant ([C], [F], and [I]) tissues. In situ hybridization was carried out using ^{33}P-labeled probes (A) and digoxigenin-labeled probes ([D] and [G]). β-galactosidase activity identified cells that expressed TWH in the TWH $^{(+/-)}$ heterozygote and had an active TWH promoter (TAP cells) in the TWH$^{(-/-)}$ mutant.

(A–C) Coronal sections of E12.5 midbrain. TWH is expressed in the hypothalamus and tectum.

(D–F) Coronal sections of E14.5 midbrain. TWH is expressed in the mammilary body and ventrolateral hypothalamus.

(G–I) Transverse sections of E14.5 thoracic spinal cord. TWH is expressed in ependymal cells lining the central canal and in a subset of ventral cells.

(J–L) Whole-mount staining of E10.5 embryos (J) and E18.5 brains ([K] shows ventral surface; [L] shows dorsal surface) for β-galactosidase activity. A TWH$^{(-/-)}$ mutant is on the right; a TWH$^{(+/-)}$ heterozygote is on the left. The TWH$^{(-/-)}$ mutant brain had a smaller group of TAP cells in the lateral hypothalamus (arrow in [K]) and pretectal region (arrow in [L]). Scale bars = 400 μm, (A–C); 100 μm, (D–F); 50 μm, (G–I); 685 μm, (J); 1.5 μm, (K); and 1.0 μm, (L).

the morphology and staining pattern of these cells suggest that they represent glial cells. An occasional TAP glial cell was found in the ventral spinal cord (Figure 3G).

TAP Motor Neurons Constitute Subsets of the MMCm and the LMCl

To understand the potential role of TWH in the development of spinal cord neurons, we examined its pattern of expression at earlier stages. TWH is initially expressed throughout the neuroepithelium of the developing spinal cord (Figure 1J; data not shown). TWH is therefore expressed in all neural progenitors that will give rise to motor neurons and ventral interneurons. TAP motor neurons could be identified among the newly generated motor neurons by E10.5–E11.5, and TAP interneurons could be identified by E12.5 (data not shown). The nascent TAP motor neurons were difficult to classify as MMC or LMC neurons because of their continued migration within the spinal cord at these times. We therefore analyzed TAP motor neurons at E13.5, after motor neurons have settled close to their final positions within the spinal cord (Figure 4).

The location of TAP motor neurons in the E13.5 spinal cord was similar to that found at E18.5. TAP motor neurons constituted subsets of both the MMC and LMC (Figures 4A–4D). At thoracic levels, the MMC can be divided into a medial and lateral subdivision. Motor neurons in the medial MMC (MMCm) project to axial muscles derived from the dorsal mesenchyme, while motor neurons found in the lateral MMC (MMCl) project to axial

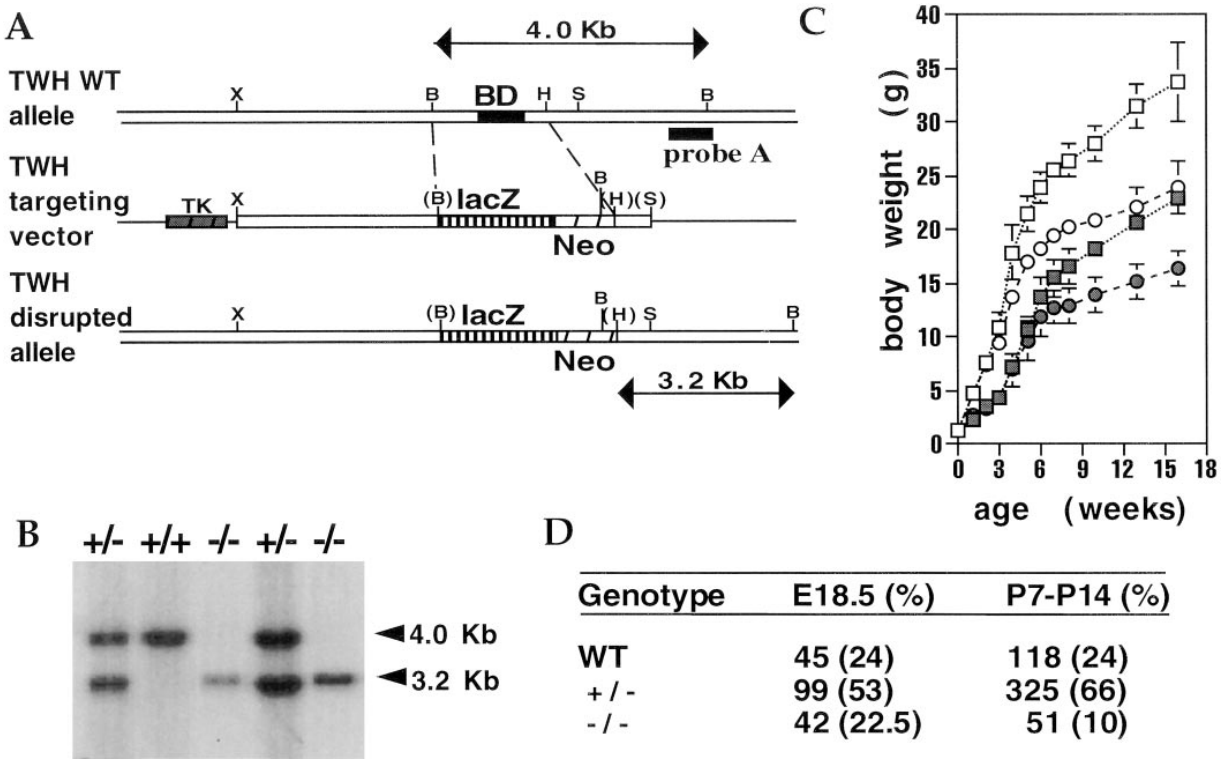

Genotype	E18.5 (%)	P7-P14 (%)
WT	45 (24)	118 (24)
+ / -	99 (53)	325 (66)
- / -	42 (22.5)	51 (10)

Figure 2. Targeted Disruption of the TWH Gene

(A) The targeting vector, wild-type TWH allele, and disrupted TWH allele after homologous recombination are shown. Expression of the lacZ cassette is under the control of the TWH promoter. B, BamHI; H, HpaI; S, SmaI; and X, XhoI. BD, binding domain; lacZ, lacZ cassette; Neo, neomycin resistance cassette; and TK, thymidine kinase cassette. Parentheses indicate loss of restriction enzyme site.

(B) Southern blot analyses of tail DNAs from wild-type $^{(+/+)}$, TWH$^{(+/-)}$, and TWH$^{(-/-)}$ mice, using the probe shown in (A).

(C) TWH$^{(-/-)}$ mutant mice fail to thrive postnatally. Mice from TWH$^{(+/-)}$ heterozygous matings were followed for 18 weeks, with animals weighed at weekly intervals. Mice were genotyped at 1 week of age. No difference in weight was found at birth, but differences were readily apparent by 1 week of age. After the TWH$^{(-/-)}$ mutant mice were weaned at 3–4 weeks, they grew at a normal rate. Data of the WT animals are not shown but were similar to the TWH$^{(+/-)}$ heterozygote data. 6 WT males, 4 WT females, 14 TWH$^{(+/-)}$ heterozygous males (open squares), 10 TWH$^{(+/-)}$ heterozygous females (open circles), 10 TWH$^{(-/-)}$ mutant males (closed squares), and 8 TWH$^{(-/-)}$ mutant females (closed circles) were followed. SDs are shown.

(D) TWH$^{(-/-)}$ mutants have reduced survival postnatally. Normal numbers of TWH$^{(-/-)}$ mutant mice were found at the end of gestation (E18.5), but less than half of the expected numbers were found by P7–P14.

muscles derived from the ventral mesenchyme (Gutman et al., 1993; Tsuchida et al., 1994). In the chick, motor neurons of the MMCm can be distinguished from those of the MMCl by their expression of the LIM homeobox transcription factor Lim-3 (Tsuchida et al., 1994). Preliminary studies indicate that this same pattern of LIM gene expression distinguishes motor neurons in the mouse (Pfaff and Jessell, unpublished data). We found that at thoracic levels, TAP motor neurons were located in the medial half of the MMC (Figure 4B), and that they, similar to other medial MMC motor neurons, expressed Lim-3 (Figures 5A–5C).

The LMC can also be divided into medial and lateral subgroups, with motor neurons in the medial LMC subdivision projecting to ventral mesenchyme–derived limb muscles and motor neurons in the lateral LMC subdivision projecting to dorsal mesenchyme–derived limb muscles. TAP motor neurons were positioned in the lateral half of the LMC, suggesting that they formed a subset of the LMCl (Figure 4C). We again used antibodies to chick LIM homeobox factors to distinguish these motor column subsets. Chick LMCl motor neurons, but not LMCm motor neurons, express Lim-1 (Tsuchida et al., 1994). TAP LMC motor neurons, as well as other motor neurons in the lateral LMC, stained with pan-Islet and Lim-1 (Figures 4C and 5G–5I). Thus, TAP LMC motor neurons express markers characteristic for LMCl motor neurons.

TAP Motor Neurons Are Confined to Specific Spinal Cord Segments

Motor neurons of the medial motor column are distributed along the entire length of the spinal cord, with their greatest numbers concentrated at thoracic and cervical levels. LMC motor neurons are restricted to the lower cervical (brachial) and lumbar levels, with peak numbers located at midbrachial and midlumbar levels (Hollyday and Hamburger, 1977). We surveyed E13.5 and E18.5 spinal cords to determine the A–P distribution of TAP motor neurons. TAP motor neurons found in the medial motor column were concentrated at thoracic and lumbar levels (Figures 4B–4D). Very few TAP motor neurons

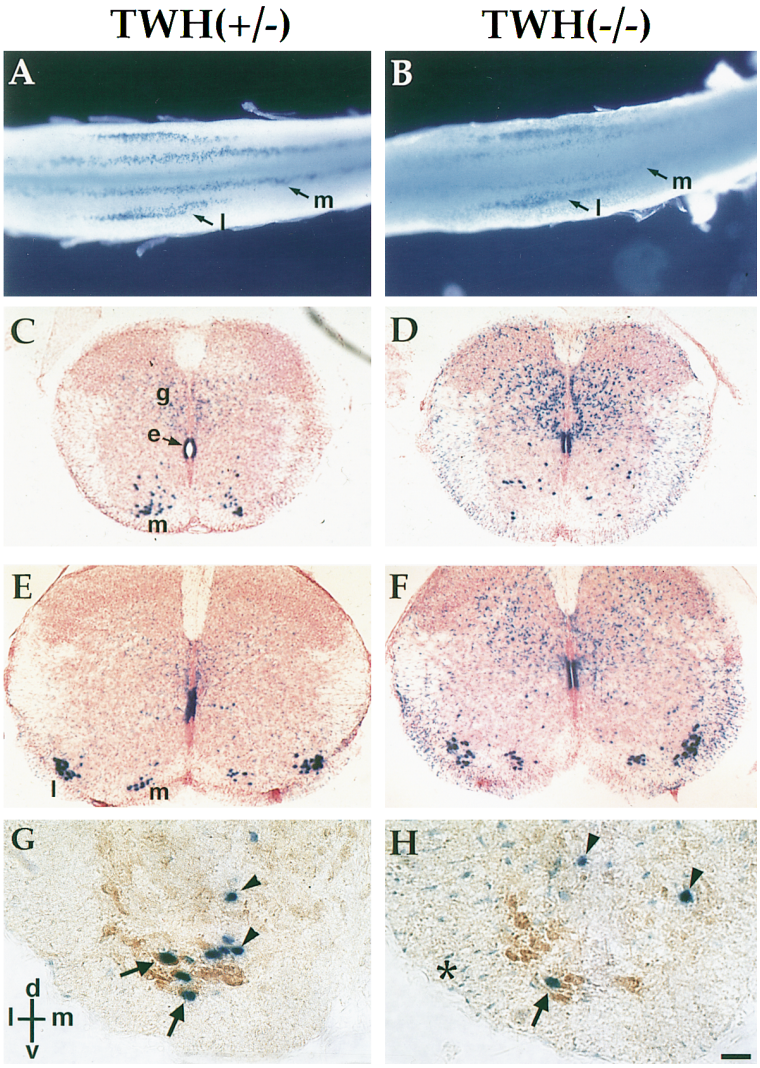

Figure 3. The TWH$^{(-/-)}$ Mutant Has an Altered Pattern of TAP (TWH Active-Promoter) Neural Cells in the Spinal Cord

(A and B) Whole-mount staining of E18.5 spinal cord for β-galactosidase activity. Arrows point to the medial (m) and lateral (l) longitudinal columns of TAP cells that were found on the ventral surface. The anterior end of the spinal cord is to the right, the posterior to the left.

(C–F) Transverse sections of E18.5 spinal cord (75 μm), stained for β-galactosidase activity and counterstained with nuclear fast red. TAP cells found in the medial (m) and lateral (l) ventral columns were identified as interneurons and motor neurons by immunohistochemistry. Additional TAP cells were identified as ependymal cells (e) and glial cells (g). The TWH$^{(-/-)}$ mutation affected the distribution and numbers of the TAP neuronal and glial populations.

(C and D) Transverse sections at midthoracic levels.

(E and F) Transverse sections at L1–L2.

(G and H) Transverse sections of E18.5 thoracic spinal cord (15 μm), stained for β-galactosidase (blue) and acetylcholinesterase (brown) activity. All of the large ventral TAP cells were identified as neurons. Arrows point to TAP motor neurons, identified by their blue nucleus and brown cytoplasm. Arrowheads point to TAP interneurons. Many TAP glial cells (small narrow nuclei TAP cells surrounding the asterisk) were found in the TWH$^{(-/-)}$ mutant spinal cord; only a few of these cells were found in the TWH$^{(+/-)}$ heterozygote. Scale bars = 280 μm, ([A] and [B]); 100 μm, (C–F); and 25 μm, ([G] and [H]).

were found at cervical or sacral levels (Figures 4A and 4I; data not shown). TAP motor neurons therefore constituted a limited subset of the MMC along the A–P axis.

TAP motor neurons of the lateral motor column demonstrated an even more restricted pattern of distribution. TAP LMC motor neurons were exclusively located in only one of the two groups of LMC motor neurons, namely, the lumbar group (Figures 4A, 4C, and 4I). In addition, although the lumbar LMC extends from L1–L5 at E18.5 and from L1–L6 at E13.5 (Lance-Jones, 1982), TAP motor neurons were confined to the L1–L3 segments (Figures 4C and 4D).

The limited distribution of TAP motor neurons along the A–P axis resembles the pattern described for motor neuron pools. Retrograde labeling studies have demonstrated that each muscle is innervated by a pool of motor neurons. Motor neuron pools occupy specific positions within the transverse spinal cord and extend over a limited number of spinal cord segments, forming a smaller longitudinal column within the major motor columns (reviewed by Hollyday, 1980; Landmesser, 1980). Several muscles, including the quadriceps femoris, pectineus, and adductors, have their motor neurons located within the L1–L3 levels (McHanwell and Biscoe, 1981). Among these, the motor neurons that innervate the quadriceps femoris occupy the most ventrolateral region of the LMC, the same position occupied by TAP LMC motor neurons. TAP LMC motor neurons may therefore represent the quadriceps femoris motor neuron pool. No studies have been carried out on the motor neuron pools of thoracic axial muscles of the mouse. Comparisons with the pattern of thoracic axial motor neuron pools of the rat suggest that TAP thoracic motor neurons may represent the motor neuron pool for the longissimus, iliocostalis, or levator costae muscles (Smith and Hollyday, 1983).

TWH Mutant Mice Fail to Thrive Postnatally and Have Motor Weakness

Mice homozygous for the TWH mutation were indistinguishable from TWH$^{(+/-)}$ heterozygote and WT mice at birth. They were born at the expected frequency and

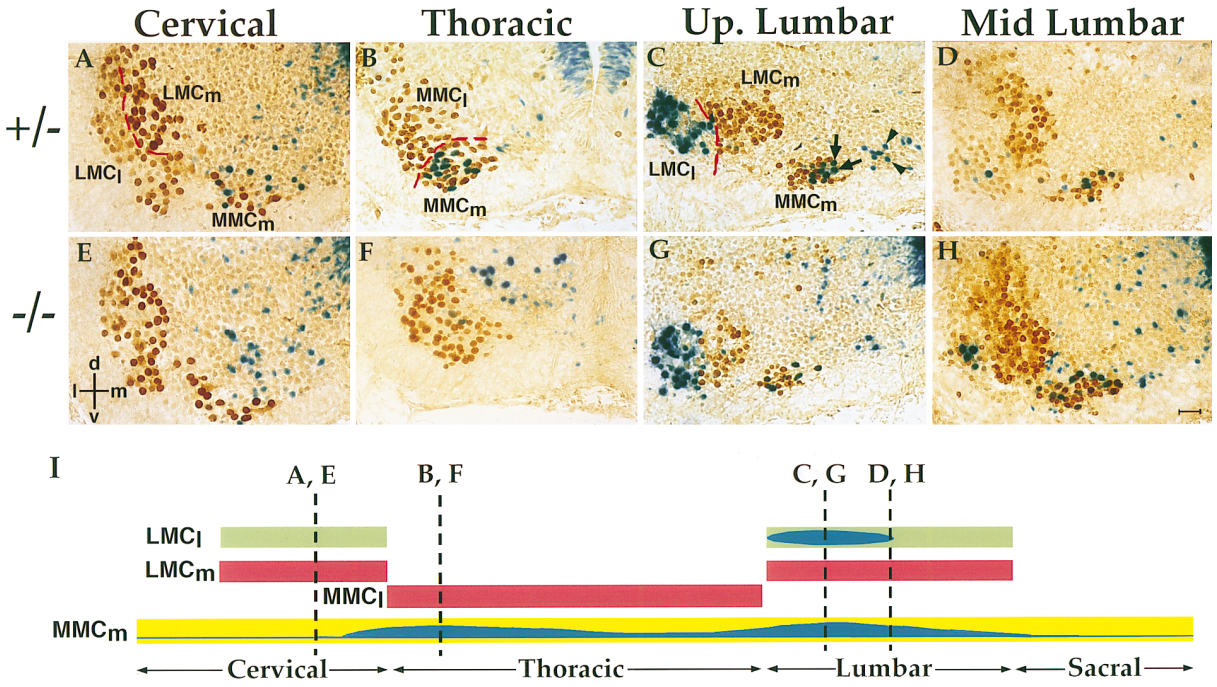

Figure 4. TAP Motor Neurons Show a Restricted Pattern of Distribution along the A–P Axis

(A–H) TAP motor neurons in E13.5 spinal cords were detected by colabeling for Islet (brown) and β-galactosidase activity (blue). TAP motor neurons were primarily found at thoracic and lumbar levels. Dashed red lines demarcate LMC_l from LMC_m motor neurons ([A] and [C]) and MMC_m from MMC_l motor neurons (B).

(A and E) Cervical (C5);

(B and F) Thoracic (T1);

(C and G) Upper lumbar (L1);

(D and H) Mid lumbar (L3).

(I) The distribution of TAP motor neurons within the different somatic motor columns is shown. Only half of the somatic spinal motor columns are depicted. The color code corresponds to the pattern of LIM homeobox gene expression found in the chick (Tsuchida et al., 1994). Yellow: Isl-1, Isl-2, Lim-3; red: Isl-1, Isl-2; and green: Isl-2, Lim-1. The location of TAP motor neurons within the different motor column is shown in blue. The thickness of the blue band indicates the relative size of the TAP motor neuron population at the different levels. TAP motor neurons were found in the MMC_m, primarily at thoracic and lumbar levels, and in the LMC_l but only at lumbar (L1–L3) levels. Arrows point to TAP motor neurons; arrowheads point to TAP interneurons. Scale bars = 25 μm. Dorsal, ventral, lateral, and medial orientations are indicated.

were of normal weight and size. Postnatally, differences between the $TWH^{(-/-)}$ mutant and their normal littermates quickly became apparent. Most $TWH^{(-/-)}$ mutant pups died within 48 hr of birth, with additional increased mortality over the first 2 weeks (Figure 2D). $TWH^{(-/-)}$ mutant pups had a markedly reduced rate of growth; by P7, $TWH^{(-/-)}$ mutant animals were half the weight of their normal littermates (Figure 2C). This reduction in growth rate persisted until the pups were weaned to solid food (3–4 weeks). $TWH^{(-/-)}$ mutant mice consumed normal amounts of solid food per gram of body weight, and their growth rate paralleled that found in $TWH^{(+/-)}$ heterozygote and WT mice after 4 weeks of age (Figure 2C; data not shown). However, $TWH^{(-/-)}$ mutant mice never completely recovered from their initial growth retardation and always remained smaller than their littermates. $TWH^{(-/-)}$ mutant animals that survived the perinatal period appear to have a normal life span and were fertile.

$TWH^{(-/-)}$ mutant mice were noted to have decreased gross motor activity; they explored their cage less often and did not move as rapidly as their normal littermates. WT and $TWH^{(+/-)}$ heterozygote mice darted away when touched, while some $TWH^{(-/-)}$ mutant mice made no attempt to escape and only responded by vocalization. Additionally, some $TWH^{(-/-)}$ mutants displayed a broad based gait (Figure 6A) and an abnormal clutching reflex (Figure 6C). No sensory deficits were detected in the $TWH^{(-/-)}$ mutant mice. Responses to either a noxious (tail pinch assay) or a thermal stimulus (tail flick and hot plate assays) were normal (data not shown).

Motor strength was evaluated by a modified grasp test. Animals were placed onto a horizontal rod, which they grasped with all four limbs. Mice were scored according to the length of time that they could support their weight from the rod. This test assessed motor strength in both fore- and hindlimbs as well as the trunk. Most WT and $TWH^{(+/-)}$ heterozygote mice supported their weight for 60 s or more, while 80% of the $TWH^{(-/-)}$ mutant mice failed to support their weight for >20 s (Figure 6D). No differences were noted in motor strength upon repeated testing over 4 months. $TWH^{(-/-)}$ mutant animals that had a poor grasp time at an early age continued to have a poor time at older ages, while the few $TWH^{(-/-)}$ mutant animals that could initially support their weight for 60 s or more remained strong. Because all of the animals were growing progressively larger over this period, we could conclude that the size of the mice was not a

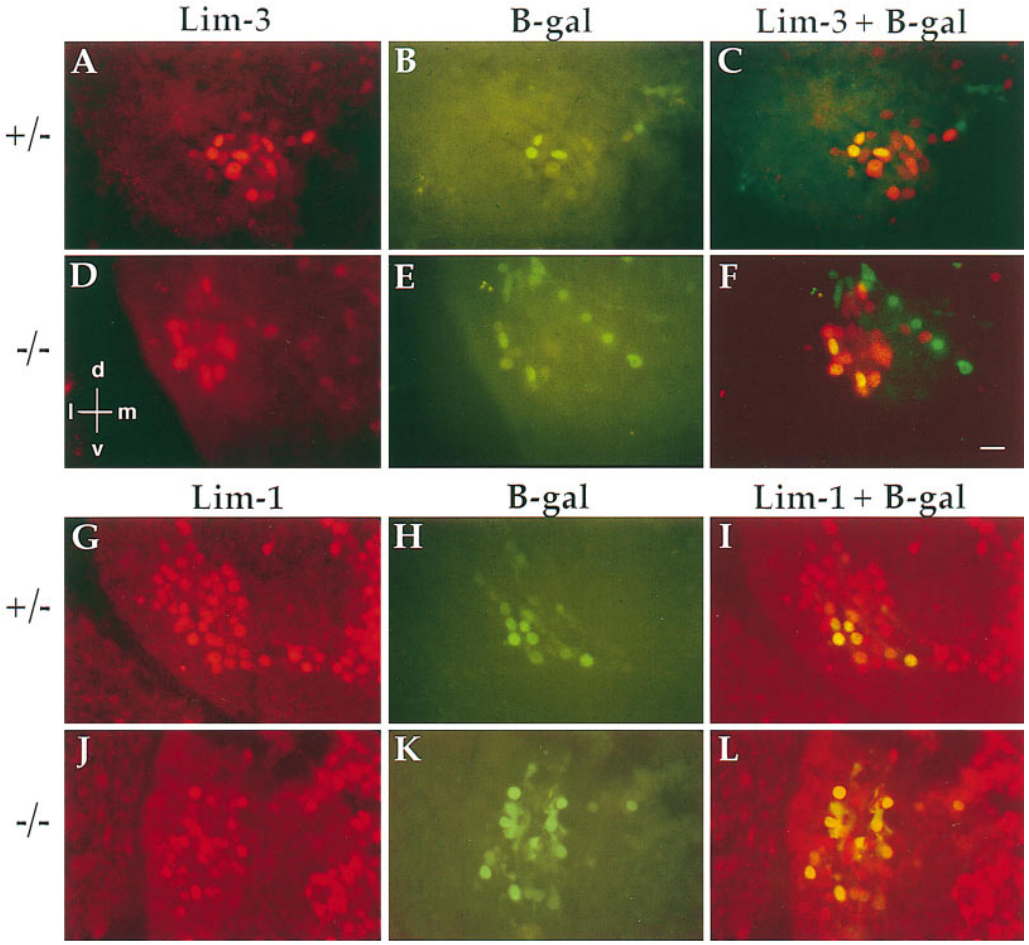

Figure 5. TAP Motor Neurons Express Lim Genes

Coexpression of Lim-3 or Lim-1 homeobox genes and β-galactosidase protein determined by double-labeling immunohistochemistry on E13.5 spinal cord sections. Lim genes were detected with anti-Lim-3 or T4 and a Cy-3 conjugated secondary antibody (red). β-galactosidase protein was detected with anti-β-galactosidase antibody and an FITC-conjugated secondary antibody (green). Double-labeled cells are yellow (Lim-3^+/β-gal^+, [C] and [F]; Lim-1^+/β-gal^+, [I] and [L]). The scale bar = 25 μm.

variable that affected their strength. These findings suggest that the $TWH^{(-/-)}$ mutant mice have a neuromuscular deficit. We cannot exclude the possibility that the mutant mice also have localized sensory deficits.

The lacZ Marker Identifies TAP Neural Cells in the $TWH^{(-/-)}$ Mutant Animal

No abnormalities in the morphology of the mutant embryos were readily apparent by gross examination or light microscopy. We therefore specifically examined the tissues and cells that expressed TWH in order to understand how the disruption of the TWH gene contributed to the observed motor weakness. We compared the pattern of β-galactosidase activity in $TWH^{(-/-)}$ mutant versus $TWH^{(+/-)}$ heterozygous tissues (Figures 1C, 1F, and 1I versus Figures 1B, 1E, and 1H) and to in situ hybridization studies of WT tissues (Figures 1A, 1D, and 1G). Staining patterns were similar, indicating that the lacZ reporter identifies in the $TWH^{(-/-)}$ mutant the same population of cells that expresses TWH in WT and heterozygous embryos.

No differences in the pattern of TAP cells were found between the $TWH^{(+/-)}$ heterozygote and $TWH^{(-/-)}$ mutant brains before E12.5. β-galactosidase activity was initially expressed throughout the neuroepithelium, posterior to the future telencephalon (Figure 1J; data not shown). After E12.5, subtle differences in the pattern of TAP cells were detected between the $TWH^{(-/-)}$ mutant and $TWH^{(+/-)}$ heterozygote brains in the hypothalamus and pretectal regions (Figures 1K and 1L; data not shown). No TAP cells were found in the basal ganglia or cerebral cortex of either the $TWH^{(-/-)}$ mutant or $TWH^{(+/-)}$ heterozygous brain (data not shown).

The $TWH^{(-/-)}$ Mutant Mouse Has Alterations in TAP Neural Spinal Cord Populations

Whole-mount staining for β-galactosidase activity revealed several differences in the pattern of TAP cells between the $TWH^{(-/-)}$ mutant and $TWH^{(+/-)}$ heterozygous E18.5 spinal cords. In the $TWH^{(-/-)}$ mutant spinal cord, the ventromedial columns of TAP cells were less prominent, and there was an increased level of β-galactosidase activity throughout the spinal cord (Figure 3B). The decreased prominence of the ventromedial columns

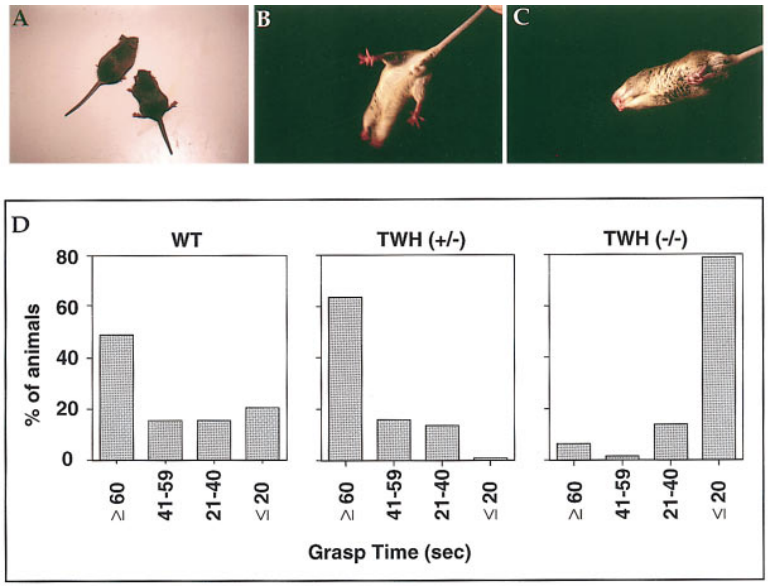

Figure 6. TWH$^{(-/-)}$ Mutant Mice Display Signs of Motor Weakness

(A) TWH$^{(-/-)}$ mutant mouse (lower right side) displays a wider-based stance than its normal TWH$^{(+/-)}$ heterozygote littermate (upper left side).

(B) TWH$^{(+/-)}$ heterozygous mouse extends its limbs and digits when picked up by its tail, while a TWH$^{(-/-)}$ mutant mouse (C) draws in its limbs when lifted by its tail (clutching reflex).

(D) TWH$^{(-/-)}$ mutant mice have decreased motor strength. Mice held onto a horizontal rod with all four extremities and were timed from when they began to fully support their weight against gravity, i.e., when they held onto the rod from the side or bottom. Most TWH$^{(-/-)}$ mutant mice failed to support their weight for >20 s. 39 WT, 46 TWH$^{(+/-)}$ heterozygous, and 65 TWH$^{(-/-)}$ mutant mice were tested. No difference was found between male and female animals.

of TAP cells was partly due to the dispersion of these cells in the TWH$^{(-/-)}$ mutant compared to their clustered arrangement in the TWH$^{(+/-)}$ heterozygote (Figures 3D and 3C). Double-labeling studies revealed that the scattered TAP neurons represented TAP interneurons; TAP MMC motor neurons were still located within the TWH$^{(-/-)}$ mutant ventral horn (Figure 3H; data not shown). No gross changes were found in the position of the TAP motor neurons of the TWH$^{(-/-)}$ mutant lumbar LMC (Figures 3F and 4F).

The increased level of β-galactosidase activity in the TWH$^{(-/-)}$ mutant spinal cord was due to an increased number and broader distribution of TAP glial cells. Most TAP glial cells were concentrated in the dorsal gray matter, similar to their position within the TWH$^{(+/-)}$ heterozygote spinal cord (Figures 3D and 3F). However, numerous small TAP cells were also found throughout the ventral gray and white matter of the TWH$^{(-/-)}$ mutant spinal cord (Figures 3D, 3F, and 3H).

The TWH$^{(-/-)}$ Mutant Has Changes in the Size of the TAP Motor Neuron Populations at Birth

The pattern of TAP motor neurons was similar between the TWH$^{(-/-)}$ mutant and TWH$^{(+/-)}$ heterozygote animal. TAP MMC motor neurons were again predominantly found at thoracic and lumbar levels, and TAP LMC motor neurons were limited to the L1–L3 levels (Figures 4E–4H). TAP motor neurons were again located in the medial half of the thoracic MMC (Figure 4F) and in the lateral half of the lumbar LMC (Figures 4G and 4H). TAP motor neurons also expressed LIM markers characteristic for the MMC_m or LMC_l subsets (Figures 5E, 5F, and 5J–5L). However, there appeared to be changes in the number of TAP motor neurons and TAP interneurons in the TWH$^{(-/-)}$ mutant compared to the TWH$^{(+/-)}$ heterozygous spinal cord at E18.5 (Figures 3D, 3F, and 3H versus Figures 3C, 3E, and 3I). We therefore counted TAP motor neuron, TAP interneuron, and total motor neuron numbers in the E18.5 ventral horn.

There was a 62% reduction of TAP thoracic motor neurons, a 44% reduction of TAP thoracic interneurons, and no alteration in non-TAP thoracic motor neurons in the TWH$^{(-/-)}$ mutant versus the TWH$^{(+/-)}$ heterozygous spinal cord (Table 1). At lumbar levels, little difference was found in the sizes of the TAP MMC motor neuron and TAP interneuron populations (Table 1). However, there was a 36% increase in TAP LMC motor neurons and a 16% decrease in non-TAP LMC motor neurons in the TWH$^{(-/-)}$ mutant (Table 1).

The Changes in TAP Motor Neuron Numbers in the TWH$^{(-/-)}$ Mutant Mice Are Present at E13.5

The changes in TAP neuron numbers found at E18.5 could reflect alterations in the generation or survival of these cells in the TWH$^{(-/-)}$ mutant. Motor neurons are generated between E9–E11.5 (Nornes and Carry, 1978; Altman and Bayer, 1984). Approximately half of these motor neurons subsequently undergo programmed cell death between E14 and birth (Lance-Jones, 1982). Motor neuron survival may be mediated by processes that regulate their access to trophic factors (reviewed by Oppenheim, 1991). We examined TWH$^{(-/-)}$ mutant spinal cords at E13.5, after the completion of motor neuron generation, and before the period of apoptosis, to assess which process was affected by the TWH mutation. Cell counts at E13.5 were determined for the upper thoracic and upper lumbar spinal cord (Table 1).

The same pattern of changes found in TAP motor neuron numbers at E18.5 were present at E13.5. There was a 49% decrease in thoracic TAP MMC motor neurons and a 52% increase in lumbar TAP LMC motor neurons in the TWH$^{(-/-)}$ mutant (Table 1). The increase in TAP LMC motor neurons was again associated with a decrease in the non-TAP LMC motor neuron population. To determine which LMC subpopulation (LMCm versus LMCl) was affected by the TWH$^{(-/-)}$ mutation, we used the LIM markers to separately identify these two groups. No difference was found in the LMCm population, but the non-TAP LMCl subpopulation was reduced

Table 1. TWH$^{(-/-)}$ Mutant Animals Have Altered Numbers of TAP Neurons in the Spinal Cord

Age and Genotype	E13.5 TWH$^{(+/-)}$	E13.5 TWH$^{(-/-)}$		E18.5 TWH$^{(+/-)}$	E18.5 TWH$^{(-/-)}$	
Thoracic	(n = 4)	(n = 5)	*P* value	(n = 4)	(n = 4)	*P* value
TAP motor neurons	188 ± 15	92 ± 12	<0.001*	81 ± 20	31 ± 7	0.011*
TAP interneurons	279 ± 35	396 ± 33	0.003*	250 ± 32	141 ± 21	0.002*
non-TAP motor neurons	1919 ± 222	1795 ± 195	0.432	440 ± 35	427 ± 12	0.550
All thoracic motor neurons	2107 ± 234	1887 ± 194	0.199	520 ± 24	458 ± 11	0.009*
Lumbar, medial	(n = 4)	(n = 4)		(n = 4)	(n = 4)	
TAP MMC motor neurons	268 ± 73	186 ± 25	0.107	87 ± 12	72 ± 16	0.150
TAP interneurons	180 ± 50	348 ± 74	0.012*	190 ± 25	190 ± 18	0.961
non-TAP MMC mn	804 ± 127	665 ± 66	0.116	124 ± 4	123 ± 11	0.875
All MMC motor neurons	1072 ± 146	851 ± 57	0.050	211 ± 9	195 ± 7	0.030*
Lumbar, lateral	(n = 4)	(n = 4)		(n = 4)	(n = 4)	
TAP LMC motor neurons	263 ± 27	401 ± 35	0.002*	177 ± 8	240 ± 17	0.003*
non-TAP LMC mn	1896 ± 130	1554 ± 171	0.020*	577 ± 24	483 ± 8	0.002*
All LMC motor neurons	2159 ± 90	1954 ± 189	0.121	755 ± 18	722 ± 10	0.030*
LMCm motor neurons	1355 ± 123	1270 ± 163	0.452			
LMCl motor neurons	804 ± 95	684 ± 49	0.049*			
non-TAP LMCl mn	541 ± 100	284 ± 45	0.008*			

The results of total counts of motor neurons, TAP (TWH-active promoter) motor neurons, and TAP interneurons found in every fourth section of E13.5 and E18.5 upper thoracic (T1-T3 at E18.5; T1-T4 at E13.5) and upper lumbar (mid-L1 to mid-L3 at E18.5; L1-L3 at E13.5) spinal cords are shown. Sections were stained for both motor neuron markers (acetylcholinesterase activity at E18.5; pan-Islet antibody at E13.5) and β-galactosidase activity. Non-TAP motor neuron numbers were determined by subtracting TAP motor neuron number from total motor neuron numbers. LMCl motor neurons were identified by staining with T4 (Lim-1/2) and K5 (pan-Islet) and their location within the ventral horn (T4 also identifies interneurons). LMCm motor neuron numbers were determined by subtracting LMCl motor neuron numbers from total LMC motor neuron numbers or by counting darkly stained K5 motor neurons (which represent Isl-1$^+$Isl-2$^+$ cells). Both methods identified the same population. Total motor neuron numbers of TWH$^{(+/-)}$ heterozygous spinal cords were found to be similar to WT numbers. At E13.5, total WT thoracic, medial lumbar, and lateral lumbar motor neuron numbers were 2298 ± 162, 1098 ± 12, 2162 ± 54, respectively; at E18.5, total motor neuron numbers were 506 ± 26, 231 ± 9, and 725 ± 27, respectively. Two WT spinal cords were counted at E13.5 and E18.5. SDs and *P* values between TWH$^{(+/-)}$ and TWH$^{(-/-)}$ values are shown. *P* values <0.05 are marked (*). mn, motor neurons.

by 48% (Table 1). These findings suggest that the TWH$^{(-/-)}$ mutation led to a change from non-TAP LMCl to TAP LMCl motor neurons.

Because the changes in TAP and non-TAP motor neuron numbers were present before the period of motor neuron apoptosis, they most likely reflect changes in the generation of these motor neurons in the TWH$^{(-/-)}$ mutant. No evidence for an earlier onset of apoptosis was detected in E11.5–E13.5 TWH$^{(-/-)}$ mutant spinal cord by the TUNEL method (Gavrieli et al. 1992) (data not shown).

TWH$^{(-/-)}$ Mutants Have an Increased Number of TAP Interneurons at E13.5

To better understand the reduction in TAP interneurons found at E18.5, we determined their numbers at an earlier age. We chose to count TAP interneurons at E13.5, as nearly all interneurons have been generated by this time (Nornes and Carry 1978). In contrast to the findings of the thoracic TAP motor neuron population, there was a 42% increase in the thoracic TAP interneuron population in the TWH$^{(-/-)}$ mutant compared to the TWH$^{(+/-)}$ heterozygote at E13.5 (Table 1). A similar anomaly was found at lumbar levels, with the TWH$^{(-/-)}$ mutant lumbar interneuron population increased by 93% compared to the TWH$^{(+/-)}$ heterozygote (Table 1). The decreased numbers of TAP interneurons found in the E18.5 TWH$^{(-/-)}$ mutant spinal cord were therefore not due to decreased generation of these neurons. Instead, this reduction most likely reflects decreased survival of these cells between E13.5–E18.5.

Discussion

WH Genes and Neural Development

The TWH gene is a member of the winged helix family of transcription factors that plays an important role in the development of the spinal cord. Several WH family members have been found to serve essential functions during neural development. BF-1 and BF-2 show complementary patterns of expression in the developing brain and eye (Tao and Lai, 1992). BF-1$^{(-/-)}$ mutant mice have a markedly reduced cerebral cortex due to decreased proliferation and premature differentiation of the telencephalic progenitor cell (Xuan et al., 1995). HNF-3β is necessary for the formation of node and notochord structures. Consequently, floor plate and motor neurons do not develop in the neural tubes of HNF-3β$^{(-/-)}$ mutant mice (Ang and Rossant 1994; Weinstein et al. 1994).

TWH is initially expressed in the neuroepithelium of the developing spinal cord. By midgestation, TWH expression is restricted to specific subsets of neural cells in the spinal cord (TAP cells), including motor neurons and ventral interneurons. We have found that animals with a disruption of the TWH gene have alterations in the numbers and positions of their TAP neurons. Thus, TWH plays a critical role in the development of subsets of spinal cord neurons.

TWH Is Essential for Normal Motor Function

Our studies demonstrate that the TWH gene is required for normal postnatal growth and development. Animals

with a null mutation of the TWH gene had reduced viability and growth postnatally. In addition, TWH$^{(-/-)}$ mutant mice had a reduction in motor strength. The grasp test results and the wide-based gait of the mutant mice suggest that they have weakness in their hindlimbs. Although we do not yet know why the TWH$^{(-/-)}$ mutant animals are weak, we suspect that the differences that we detected between the spinal cords of the TWH$^{(-/-)}$ mutant and TWH$^{(+/-)}$ heterozygote are involved. Because TWH is expressed in the neural progenitor cell as well as in differentiated TAP neural subsets, TWH could function at numerous developmental time points. Unlike the LIM homeobox protein Isl-1, which is required for the specification or earliest development of motor neurons (Pfaff et al. 1996), TWH was not required for the specification of TAP motor neurons or other TAP cells. All of the different TAP populations were present in TWH$^{(-/-)}$ mutant animals. However, we found alterations in the sizes of all of the TAP motor neuron populations as well as in the number of TAP interneurons and TAP glial cells in the TWH$^{(-/-)}$ mutant. Furthermore, the position of the TAP interneurons and TAP glia was aberrant in the mutant spinal cord. We also found that the lumbar non-TAP LMCl motor neuron population was reduced by nearly 50%. This indicates that the entire LMCl population from L1–L3 was drastically changed by the TWH mutation. Thus, the disruption of TWH affects populations of neurons other than TAP neurons, suggesting that there may be more widespread disturbances in other populations of spinal cord neurons in addition to the changes that we observe in the TAP neurons. Motor weakness in the TWH$^{(-/-)}$ mutant mice may therefore reflect the combined effects of perturbations in the TAP and non-TAP neuronal populations.

We found that the size of the TAP motor neuron populations in the TWH$^{(-/-)}$ mutant spinal cord was altered by E13.5, before the onset of the period of motor neuron apoptosis (Table 1). This is consistent with TWH playing a role in regulating the generation of these motor neurons. We did not find any evidence for a change in the time of onset of apoptosis in the TWH$^{(-/-)}$ mutant spinal cord. Because apoptotic cells are rapidly cleared, only a fraction of the dying motor neurons can be detected (Lo et al. 1995). We therefore cannot exclude the possibility that TWH also regulates the survival of TAP motor neurons. It is likely that TWH functions in the survival of the TAP interneurons, as their numbers declined in the TWH$^{(-/-)}$ mutant between E13.5–E18.5 (Table 1).

Because TWH is expressed in neural progenitor cells, TWH could regulate the size of the different TAP populations by affecting the proliferation of this progenitor. However, while the TAP MMC population was decreased, the TAP LMC motor neuron, TAP glial cell, and initially, TAP interneuron populations were increased in the TWH$^{(-/-)}$ mutant. These findings indicate that if TWH regulates the proliferation of the TAP progenitor, then it must enhance proliferation in some progenitors while inhibiting the proliferation of others.

Alternatively, the changes found among the different TAP neural subtypes in the TWH$^{(-/-)}$ mutant suggest that TWH regulates the differentiation of the TAP progenitor cell. Motor neurons are the first major spinal cord population born, followed by interneurons, and later, glial cells (Nornes and Carry 1978; Altman and Bayer 1984). In the chick, MMC motor neurons are born before LMCl motor neurons (Hollyday and Hamburger 1977; Tsuchida et al. 1994). If a similar pattern of motor neuron development occured in the mouse as in the chick, then our results suggest that TWH may regulate the responsiveness of the pluripotent TAP progenitor cell to early differentiation cues. If fewer TAP progenitor cells differentiated into MMC motor neurons, then more would remain as progenitors and continue to proliferate. This would lead to an increased number of TAP progenitors available to differentiate into the later-born TAP cells (LMCl motor neurons, interneurons, and glial cells). Also consistent with this hypothesis is the aberrant position of the TAP cells in the TWH$^{(-/-)}$ mutant. Neurons settle at specific positions in the spinal cord, with early-born cells generally settling in the ventral spinal cord and later-born populations settling in progressively more dorsal positions (Nornes and Carry 1978; Altman and Bayer 1984). The increased number and more dorsal position of TAP interneurons suggest that more cells were born at later times in the TWH$^{(-/-)}$ mutant. The recent report that a novel WH factor mediates the transcriptional response to an activin signal (Chen et al., 1996) raises the possibility that TWH may be required for spinal cord progenitors to respond to signaling molecules of the TGF-β superfamily. Several members of this family are known to function in dorsoventral patterning of the spinal cord (reviewed by Tanabe and Jessell, 1996).

TWH Identifies Unique Subsets of Motor Neurons

We have found that TWH expression identifies distinctive subsets of motor neurons. Several studies have demonstrated that the MMC and LMC and their medial and lateral subdivisions can be identified by their expression of particular combinations of LIM homeobox genes (Tsuchida et al. 1994; Appel et al. 1995). We found that TAP motor neurons were exclusively in the MMCm and LMCl motor columns. Motor neurons of the MMCm project their axons to dorsally derived axial muscles. Motor neurons of the LMCl project their axons to hip girdle and limb muscles derived from the dorsal mesenchyme. Thus, TWH expression in the MMC and LMC identified motor neurons that innervated dorsal targets.

The pattern of TWH expression differed in several respects from that of the LIM homeobox proteins. TAP motor neurons represented only a subset of the MMCm and LMCl along both the transverse and A–P axis. The restricted distribution along the A–P axis was most apparent with the TAP LMCl subpopulation. LMCl motor neurons, as identified by the LIM factor Lim-1, were found at cervical and lumbar levels, but TWH expression specifically identified lumbar LMCl motor neurons. Although cervical and lumbar LMC motor neurons innervate limb muscles, their target muscles serve different functions (i.e., weight bearing in hindlimbs versus feeding in forelimbs). The differences between their target muscles suggests that differences will be found between these two LMC motor neuron subsets. TWH is the first example of a marker that can distinguish lumbar from cervical LMC motor neurons.

The restriction of TWH expression to the lumbar and not cervical LMC motor neurons suggests that TWH expression may be under the control of genes that establish positional information along the A–P axis. Such genes include members of the Hox family of transcription factors (reviewed by Lumsden and Krumlauf, 1996). At early stages of development, manipulations of the neural tube can lead to changes in the columnar identity of motor neurons. These changes in motor neuron identity are accompanied by changes in the expression of Hox genes (Lance-Jones and Sharma, 1996, Neuroscience abstract; M. Ensini, T. Tsuchida, and T. M. Jessell, unpublished data), suggesting that the Hox genes may function in the determination of motor neuron subtype (reviewed by Tanabe and Jessell, 1996). During development, the Hox genes may restrict TWH gene expression along the A–P axis and thereby establish the positions of the TAP motor neuron subsets.

The different patterns of motor neuron expression found between TWH and members of the LIM homeobox gene family indicate that TWH, unlike the LIM genes, is not a marker of motor columns. Instead, TAP motor neurons represent specific A–P subsets of MMCm and LMCl motor neurons in a pattern that is characteristic of motor neuron pools. LIM homeobox proteins have been postulated to function in the specification of the initial pathway choices of the axons of the major motor column subsets (Tsuchida et al., 1994; Tosney et al., 1995). The restricted pattern of TWH expression suggests that TWH may function in the specification of the more distal pathway choices, such as those required to reach the target muscle of individual motor neuron pools.

Experimental Procedures

Generation of the TWH$^{(-/-)}$ Mutant Mouse

Genomic 129–SVJ clones containing the TWH gene were isolated from a λFixII library (Stratagene). LacZ and pGKNeo cassettes were used to replace the TWH BD as previously described (Hatini et al. 1996), and an HSV–TK cassette was added 5′ to the targeting sequences. A 10 kb TWH fragment was used as the 5′ targeting arm, and a 0.9 kb fragment as the 3′ arm. The targeting vector was transfected into W9.5 ES cells, and transfectants were selected with G418 (350 μg/ml) and FIAU (50 pM) as previously described (Kontgen and Stewart, 1993).

Histology and β-Gal Staining

Embryos were obtained from timed pregnancies, with noon of the plug date defined as E0.5. Embryos were fixed in 4% paraformaldehyde and processed for paraffin and cryostat sectioning as previously described (Xuan et al., 1995). Paraffin sections (8 μm) and 10–15 μm cryostat sections were collected on superfrost slides (Fisher).

Whole-mount and tissue staining for β-galactosidase activity was performed according to standard techniques (Hogan et al., 1994). To compensate for the difference in copy number of the lacZ gene, TWH$^{(+/-)}$ heterozygous tissues were stained for more than twice as long as TWH$^{(-/-)}$ mutant tissues for β-galactosidase activity. Sections were counterstained with nuclear fast red or cresyl violet.

Immunohistochemistry

Cryostat sections were processed for immunohistochemistry studies as previously described (Xuan et al., 1995). Primary antibodies were K5 rabbit anti-Islet (Isl-1/Isl-2) (Tsuchida et al., 1994), T4 rabbit anti-Lim-1/Lim-2 (Tsuchida et al., 1994), rabbit anti-Lim-3 (Ericson and Jessell), rabbit anti-GFAP (Dako), Rat-401 mouse anti-nestin (Hockfield and McKay, 1985), cyn-1 mouse anti-neuronal marker (Jessell), and goat anti-beta-galactosidase (Arnel). The secondary antibodies used were biotin-conjugated goat anti-rabbit (Vector), biotin-conjugated goat anti-mouse IgM (Southern biotechnology), peroxidase-conjugated goat anti-mouse IgG (Jackson), Cy3-labeled donkey anti-rabbit (Jackson), and FITC-labeled donkey anti-goat (Jackson). Biotin conjugated secondary antibodies were developed with peroxidase-conjugated avidin (Vectastain ABC kit, Vector) using diaminobenzidin (DAB) as substrate (Sigma). Fluorescent double-labeled sections were mounted with aqueous mounting solution (SlowFade Light, Molecular Probes) and visualized with a Zeiss III RS fluorescent microscope. Photographs were taken under rhodamine and fluorescein filters. The images were superimposed in Adobe Photoshop to identify the double-labeled cells.

Motor Neuron Cell Counts

Motor neurons were identified at E13.5 by their staining with the K5 antibody and their position within the spinal cord (Tsuchida et al., 1994). Because expression of the LIM genes decreases during late gestation (S. Pfaff, unpublished data), we used acetylcholinesterase activity to identify motor neurons at E18.5 (Karnovsky and Roots, 1964). Motor neurons can be distinguished from other cells that express acetylcholinesterase by their morphology and spinal cord position (Flanagan, 1969; Lance-Jones, 1982; Bovolenta and Dodd, 1991). Sections were stained for β-galactosidase activity following their staining for motor neuron markers. At E18.5, embryos from three TWH$^{(+/-)}$ × TWH$^{(-/-)}$ and one TWH$^{(+/-)}$ × TWH$^{(+/-)}$ litters were analyzed; at E13.5, embryos from six TWH$^{(+/-)}$ × TWH$^{(-/-)}$ and one TWH$^{(+/-)}$ × TWH$^{(+/-)}$ litters were analyzed. The parental mice were F1–F3 offspring of a 129 × C57 B6 mating. The nine TWH$^{(+/-)}$ × TWH$^{(-/-)}$ litters contained 29 TWH$^{(-/-)}$ mutant and 35 TWH$^{(+/-)}$ heterozygous embryos; the two TWH$^{(+/-)}$ × TWH$^{(+/-)}$ litters contained seven TWH$^{(-/-)}$ mutant, three WT, and six TWH$^{(+/-)}$ heterozygous embryos.

We counted cells as motor neurons if they were located in the ventral horn, had a large nucleus surrounded by visible cytoplasm, and expressed acetylcholinesterase activity in the cytoplasm at E18.5, or stained for K5 at E13.5. TAP motor neurons were counted if they met the criteria for motor neurons and stained for β-galactosidase activity. TAP interneurons were counted if they were located in the ventral half of the spinal cord, had a large nucleus, stained for β-galactosidase activity, and did not stain for motor neuron markers. Staining studies demonstrated that these cells stained for the neuronal marker cyn-1 and did not stain for glial markers GFAP or nestin. Motor neurons, TAP motor neurons, and TAP interneurons had a similar size nuclei at E13.5 and E18.5. Adjacent sections were stained only for motor neuron markers or only for β-galactosidase activity. These adjacent sets were then counted for motor neurons or TAP neurons, respectively, to verify the accuracy of the double-staining counts. Both sides of the spinal cord were counted, and no correction was made for split nuclei. At each age, the same number of sections were counted for WT, TWH$^{(+/-)}$, and TWH$^{(-/-)}$ mutant spinal cords. Positions were identified by counting the dorsal root ganglia and confirmed by analyzing the pattern of the motor columns (i.e., LMC versus MMC).

In Situ Hybridization

Cryostat sections were processed for in situ hybridization using digoxigenin-labeled or ^{33}P-labeled RNA probes as previously described (Wilkinson, 1992; Xuan et al., 1995). A plasmid containing 600 bp from the 3′ portion of the TWH cDNA was linearized and transcribed with T7 RNA polymerase using digoxigenin-labeled (Boehringer Mannheim) or ^{33}P-labeled nucleotides (NEN). Probes were detected with anti-digoxigenin antibody (Boehringer Mannheim) or by exposure to Kodak NTB-2 nuclear emulsion for 5–7 days at 4°C followed by Kodak D-19 developer. Sections were counterstained with hematoxylin and eosin.

Behavioral Analysis

Motor strength was assayed on mice 4 weeks of age and older by a modification of a grasp strength test (Lee et al., 1994). Animals supported their weight by holding onto a horizontal rod with all four limbs and were scored according to the length of time that they

remained suspended. The best score of three trials was used, and mice were retested on separate days. At least one tester was blinded as to the mouse's genotype. Sensory tests were carried out on animals prior to their being genotyped. Response to noxious stimuli was assayed by the tail pinch test (Crowley et al., 1994) carried out on P1–P7 mice. 29 WT, 35 TWH$^{(+/-)}$, and 22 TWH$^{(-/-)}$ were studied; all responded by vigorous squirming and vocalization. Response to thermal pain was assayed by a tail flick assay (55°C) and a hot plate assay (52°C) carried out on 4- to 6-week-old mice (Crowley et al. 1994). 10 WT, 32 TWH$^{(+/-)}$, and 17 TWH$^{(-/-)}$ were studied; all gave similar response times.

Acknowledgments

Address correspondance to S. L. We thank Kawai Oneda and Gabriela Balas for expert technical assistance and Vera D. Soares for blastocyst injections. We thank A. J. Silverman for sharing equipment and help with the analysis of TWH expression in the brain, and T. M. Jessell, S. Pfaff, S. Morgan, and C. Mason for providing antibodies and communicating unpublished studies. We thank T. M. Jessell, S. Pfaff, J. Dodd, A. J. Silverman, C. Mason, R. Marcus, D. Hirsh, and members of the Hirsh laboratory for helpful discussions. We are grateful to T. M. Jessell, C. Mason, and D. Hirsh for their critical comments on the manuscript. This work was supported by grants from the American Cancer Society and March of Dimes (Basil O'Connor Starter Scholar Award) to S. L.; and NIH grants to E. L. (No. RO1HD29584), to C. D. (T32 DK07313), and to Memorial Sloan-Kettering Cancer Center (Cancer Center Support Grant).

Received January 7, 1997; revised March 21, 1997.

References

Altman, J., and Bayer, S.A. (1984). The development of the rat spinal cord. Adv. Anat. Embryol. Cell Biol. *85*, 1–164.

Ang, S., and Rossant, J. (1994). HNF-3β is essential for node and notochord formation in mouse development. Cell *78*, 561–574.

Ang, S.-L., Wierda, A., Wong, D., Stevens, K.A., Cascio, S., Rossant, J., and Zaret, K.S. (1993). The formation and maintenance of the definitive endoderm lineage in the mouse: involvement of HNF3/*forkhead* proteins. Development *119*, 1301–1315.

Appel, B., Korzh, V., Glasgow, E., Thor, S., Edlund, T., Dawid, I.B., and Eisen, J.S. (1995). Motoneuron fate specification revealed by patterned LIM homeobox gene expression in embryonic zebrafish. Development *121*, 4117–4125.

Bovolenta, P., and Dodd, J. (1991). Perturbation of neuronal differentiation and axon guidance in the spinal cord of mouse embryos lacking a floor plate: analysis of Danforth's short-tail mutation. Development *113*, 625–639.

Chen, X., Rubock, M.J., and Whitman, M. (1996). A transcriptional partner for MAD proteins in TGF-β signalling. Nature *383*, 691–696.

Crowley, C., Spencer, S.D., Nishimura, M.C., Chen, K.S., Pitts-Meek, S., Armanini, M.P., Ling, L.H., McMahon, S.B., Shelton, D.L., Levinson, A.D., and Phillips, H.S. (1994). Mice lacking nerve growth factor display perinatal loss of sensory and sympathetic neurons yet develop basal forebrain cholinergic neurons. Cell *76*, 1001–1011.

Eisen, J.S. (1994). Development of motoneuronal phenotype. Annu. Rev. Neurosci. *17*, 1–30.

Flanagan, A.E.H. (1969). Differentiation and degeneration in the motor horn of the foetal mouse. J. Morphol. *129*, 281–306.

Gavrieli, Y., Sherman, Y., and Ben-Sasson, S. (1992). Identification of programmed cell death in situ via specific labeling of nuclear DNA fragmentation. J. Cell Biol. *119*, 493–501.

Grossniklaus, U., Pearson, R.K., and Gehring, W.J. (1992). The *Drosophila sloppy paired* locus encodes two proteins involved in segmentation that show homology to mammalian transcription factors. Genes Dev. *6*, 1030–1051.

Gutman, C.R., Ajmera, M.K., and Hollyday, M. (1993). Organization of motor pools supplying axial muscles in the chicken. Brain Res. *609*, 129–136.

Hatini, V., Huh, S., Herzlinger, D., Soares, V.C., and Lai, E. (1996). Essential role of stromal mesenchyme in kidney morphogenesis revealed by targeted disruption of Winged-Helix transcription factor, BF-2. Genes Dev. *10*, 1467–1478.

Hockfield, S., and McKay, R.D.G. (1985). Identification of major cell classes in the developing mammalian nervous system. J. Neurosci. *5*, 3310–3328.

Hogan, B., Beddington, R., Constantini, F., and Lacy, E. (1994). In Manipulating the Mouse Embryo. (Cold Spring Harbor, New York: Cold Spring Harbor Laboratory Press).

Hollyday, M. (1980). Motoneuron histogenesis and the development of limb innervation. Curr. Top. Dev. Biol. *15*, 181–215.

Hollyday, M., and Hamburger, V. (1977). An autoradiographic study of the formation of the lateral motor column in the chick embryo. Brain Res. *132*, 197–208.

Kaestner, K., Lee, K., Schlöndorff, J., Hiemisch, H., Monaghan, A., and Schütz, G. (1993). Six members of the mouse forkhead gene family are developmentally regulated. Proc. Natl. Acad. Sci. USA *90*, 7628–7631.

Kaestner, K.H., Schütz, G., and Monaghan, A.P. (1996). Expression of the winged helix genes *fkh*-4 and *fkh*-5 defines domains in the central nervous system. Mech. Dev. *55*, 221–230.

Karnovsky, M.J., and Roots, L. (1964). A "direct-coloring" thiocholine method for cholinesterases. J. Histochem. Cytochem. *12*, 219–221.

Kontgen, F., and Stewart, C. (1993). Simple screening procedure to detect gene targeting events in embryonic stem cells. *Guide to Techniques in Mouse Development*. (San Diego, California: Academic Press), pp. 878–890.

Lai, E., Clark, K.L., Burley, S.K., and Darnell, J.E. (1993). Hepatocyte nuclear factor-3/fork head or "winged helix" proteins: a family of transcription factors of diverse biologic function. Proc. Natl. Acad. Sci. USA *90*, 10421–10423.

Lance-Jones, C. (1982). Motoneuron cell death in the developing lumbar spinal cord of the mouse. Dev. Brain Res. *4*, 473–479.

Landmesser, L.T. (1980). The generation of neuromuscular specificity. Annu. Rev. Neurosci. *3*, 279–302.

Lee, M.K., Marszalek, J.R., and Cleveland, D.W. (1994). A mutant neurofilament subunit causes massive selective motor neuron death: implications for the pathogenesis of human motor neuron Disease. Neuron *13*, 975–988.

Lo, A.C., Houenou, L.J., and Oppenheim, R.W. (1995). Apoptosis in the nervous system: morphological features, methods, pathology, and prevention. Arch. Histol. Cytol. *58*, 139–149.

Lumsden, A., and Krumlauf, R. (1996). Patterning the vertebrate neuraxis. Science *274*, 1109–1115.

McConnell, S.K. (1995). Strategies for the generation of neuronal diversity in the developing central nervous system. J. Neurosci. *15*, 6987–6998.

McHanwell, S., and Biscoe, T.J. (1981). The localization of motoneurons supplying the hindlimb muscles of the Mouse. Philos. Trans. R. Soc. Lond. [Biol.] *293*, 477–508.

Miller, L.M., Gallegos, M.E., Morisseau, B.A., and Kim, S.K. (1993). *lin-31*, a Caenorhabditis elegans HNF-3/fork head transcription factor homolog, specifies three alternative cell fates in vulval development. Genes Dev. *7*, 933–947.

Moynahan, M.E., Akgun, E., and Jasin, M. (1996). A model for testing recombinogenic sequences in the mouse germline. Hum. Mol. Gen. *5*, 875–886.

Nornes, H.O., and Carry, M. (1978). Neurogenesis in spinal cord of mouse: an autoradiographic analysis. Brain Res. *159*, 1–16.

Oppenheim, R.W. (1991). Cell death during development of the nervous system. Annu. Rev. Neurosci. *14*, 453–501.

Pfaff, S.L., Mendelsohn, M., Stewart, C.L., Edlund, T., and Jessell, T.M. (1996). Requirement for LIM homeobox gene *Isl1* in motor neuron generation reveals a motor neuron-dependent step in interneuron differentiation. Cell *84*, 309–320.

Sasaki, H., and Hogan, B. (1993). Differential expression of multiple

fork head related genes during gastrulation and axial pattern formation in the mouse embryo. Development *118*, 47–59.

Smith, C.L., and Hollyday, M. (1983). The development and postnatal organization of motor nuclei in the rat thoracic spinal cord. J. Comp. Neurol. *220*, 16–28.

Tanabe, Y., and Jessell, T.M. (1996). Diversity and pattern in the developing spinal cord. Science *274*, 1115–1123.

Tao, W., and Lai, E. (1992). Telencephalon-restricted expression of BF-1, a new member of the HNF-3/*fork head* gene family in the developing rat brain. Neuron *8*, 957–966.

Tosney, K.W., Hotary, K.B., and Lance-Jones, C. (1995). Specifying the target identity of motoneurons. BioEssays *17*, 379–382.

Tsuchida, T., Ensini, M., Morton, S.B., Baldassare, M., Edlund, T., Jessell, T.M., and Pfaff, S.L. (1994). Topographic organization of embryonic motor neurons defined by expression of LIM homeobox genes. Cell *79*, 957–970.

Weinstein, D.C., Ruiz i Altaba, A., Chen, W.S., Hoodless, P., Prezioso, V.R., Jessell, T.M., and Darnell, J.J.E. (1994). The winged-helix transcription factor *HNF-3*β is required for notochord development in the mouse embryo. Cell *78*, 575–588.

Wilkinson, D. (1992). In situ hybridization: a practical approach. (Oxford: Oxford University Press).

Xuan, S., Baptista, C., Balas, G., Tao, W., Soares, V., and Lai, E. (1995). Winged helix transcription factor BF-1 is essential for the development of the cerebral hemispheres. Neuron *14*, 1141–1152.

GenBank Accession Number

The Genbank accession number for the full-length sequence of TWH is U90538.